ANNALS OF GEOPHYSICS, 66, 1, SE103, 2023; doi:10.4401/ag-8805
OPEN ACCESS

1D crustal structure of Albania region

Edmond Dushi[*,1] and Jens Havskov[2]

(1) Department of Seismology, Institute of Geosciences, Polytechnic University of Tirana, Albania
(2) Department of Earth Science, University of Bergen, Norway

Article history: received February 15, 2022; accepted February 6, 2023

Abstract

A new crustal 1D layered model for Albania has been determined. The data used consist of P and S readings from 108 evenly distributed and well located earthquakes using the Albanian Seismic Network and nearby seismic stations. The method used was to relocate the data using many thousand models, which were varied in a systematic way in a wide range around a start model determined from currently available models. The model with the lowest average travel time residual RMS was then selected as a final model. Tests with synthetic data showed this to be a robust method. With the dataset, the average RMS was reduced from 0.69s, using the current model, to 0.56s using the start model and to 0.49s using the final model. The new hypocenters were also found to be closer to a set of well located ISC hypocenters than the original locations. The final model found is:

Depth to interface (km)	P-velocity (km/s)
0	5.5
12	6.0
23	6.3
41	7.7

with a $V_p/V_s = 1.81$. This final model is different from the currently used model in Albania and should therefore represent a significant improvement for earthquake location.

Keywords: Seismicity and tectonics; Composition and structure of the continental crust; Crustal structure; Albania, Earthquake location

1. Introduction

Albania is a country with moderate seismicity, the latest being the magnitude M_W6.4 event in November 26, 2019 at 02:54 UTC, located 17 km north of Durres Town (41.4593N ; 19.4418E), at a depth of 39.5 km [Moshou et al., 2019 ; Dushi et al., 2020]. However, varying depth values were reported by different seismological agencies, suggesting an ambiguous relation between the November 2019 earthquake and the blind reverse fault, rooted at the basal thrust front in the foreland basin [Lekkas et al., 2019; Papadopoulos et al., 2020; Handy et al., 2020; Mavroulis et al., 2021]. To be able to make the most accurate earthquake locations it is therefore important to have the best crustal model possible. The crustal structure of Albania is not well known although some preliminary studies have been carried out. The depth to Moho has been given between 30 and 50 km and earthquakes have been located

with quite different models over the years, probably resulting in some inconsistency in their locations. In this study we will make a summary of what is known of the crustal structure and propose a new 1D model. The model will be improved by grid search testing. This consists in locating a set of earthquakes with many different models varied in a systematic way and finding the models with the average lowest RMS travel time residual.

2. Seismic network of Albania

The monitoring of earthquakes in Albania started in 1968, with the first seismological station in Tirana (TIR). The Albanian Seismological Network (ASN), which included 12 peripheral remote and one master station in Tirana [Muço 1996, 1998, 1999], officially started in 1976 and earthquakes were located manually until 2001 [Duni et al. 2003]. All the remote stations were equipped with 3-C short period (SP) seismographs.

In 2002, the first digital recording units started to be installed, still composed of 3-C, SP geophones (0.2 sec period), having a 16 bit of resolution datalogger and recording at 100 samples per sec. Data were collected through a phone dial up connection at the processing centre. A change was initiated in 2003 when the first broadband sensors started operation and data transmission was through very small aperture telemetered system (VSAT), which ensured reliable and continuous seismic recording for nearly two decades.

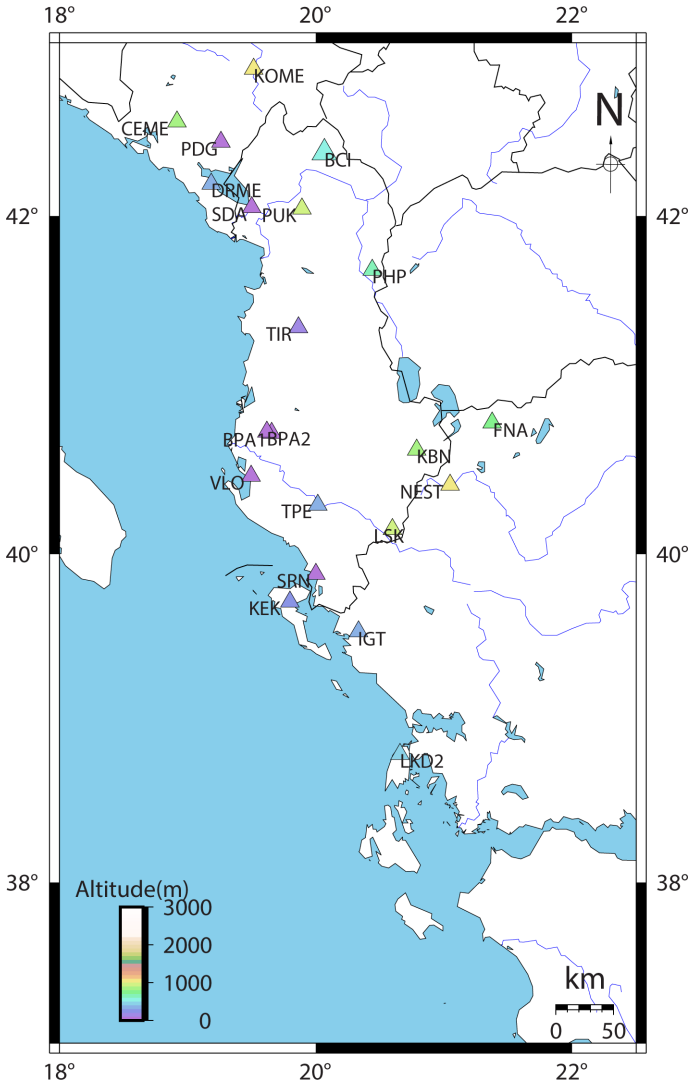

Figure 1. Stations from the Albanian seismic network, Aristotle University of Thessaloniki seismic network (stations FNA, IGT, NEST, LDK2), MedNet Project Partner Institutions (stations KEK, TIR, PDG) and Institute of Hydrometeorology and Seismology of Montenegro (stations KOME, DRME and CEME), used in this study.

The present-day seismic monitoring in Albania is based on a set of ten broadband seismic stations [Institute of Geosciences, Energy, Water and Environment, 2002], constituting the ASN (Figure1). In the normal monitoring routine of ASN, some stations from the seismic network of the Aristotle University of Thessaloniki [1981], Euro-Mediterranean seismic network of the MedNet Project Partner Institutions [1990] and Montenegrin seismic network of the Sector for Seismology, Institute of Hydrometeorology and Seismology of Montenegro [1982], are included. In the present study we use FNA, KEK, IGT, NEST and LKD2, located south of the southern Greek-Albanian border and DRME, PDG, CEME and COME, located north of the northern Montenegro-Albanian border (Figure 1).

3. Tectonic environment

Albania belongs to the Dinarides [Aliaj 1998; Meço et al. 2000; Aliaj 2006; Handy et al. 2019] forming the southern branch of the Alpine fold and thrust belt (Figure 2). This tectonic structure extends along the eastern coast of the Adriatic microplate (Adria Microplate), divided by the Shkodra-Peja (SP) transverse fault zone (Figure 2a), into two major tectonic structures: the Dinarides and the Hellenides [Aliaj 2006; Handy et al. 2019]. The Hellenides is located in Albania and Greece, along the southern convergent margin of the Eurasian plate where two segments are divided by the Cephalonia transform fault namely, the northern one belonging to the Adriatic continental collision and the southern one belonging to the Aegean arc (Hellenic), related to the active oceanic subduction [Aliaj 2006; Mihaljevic et al. 2017; Halpaap et al. 2018]. In the northern segment, along the northeastern and eastern coast of the Adriatic Sea and eastern coast of Ioanian Sea, the Adriatic-Eurasian collision has led to the build up of the Dinaric-Albanian-

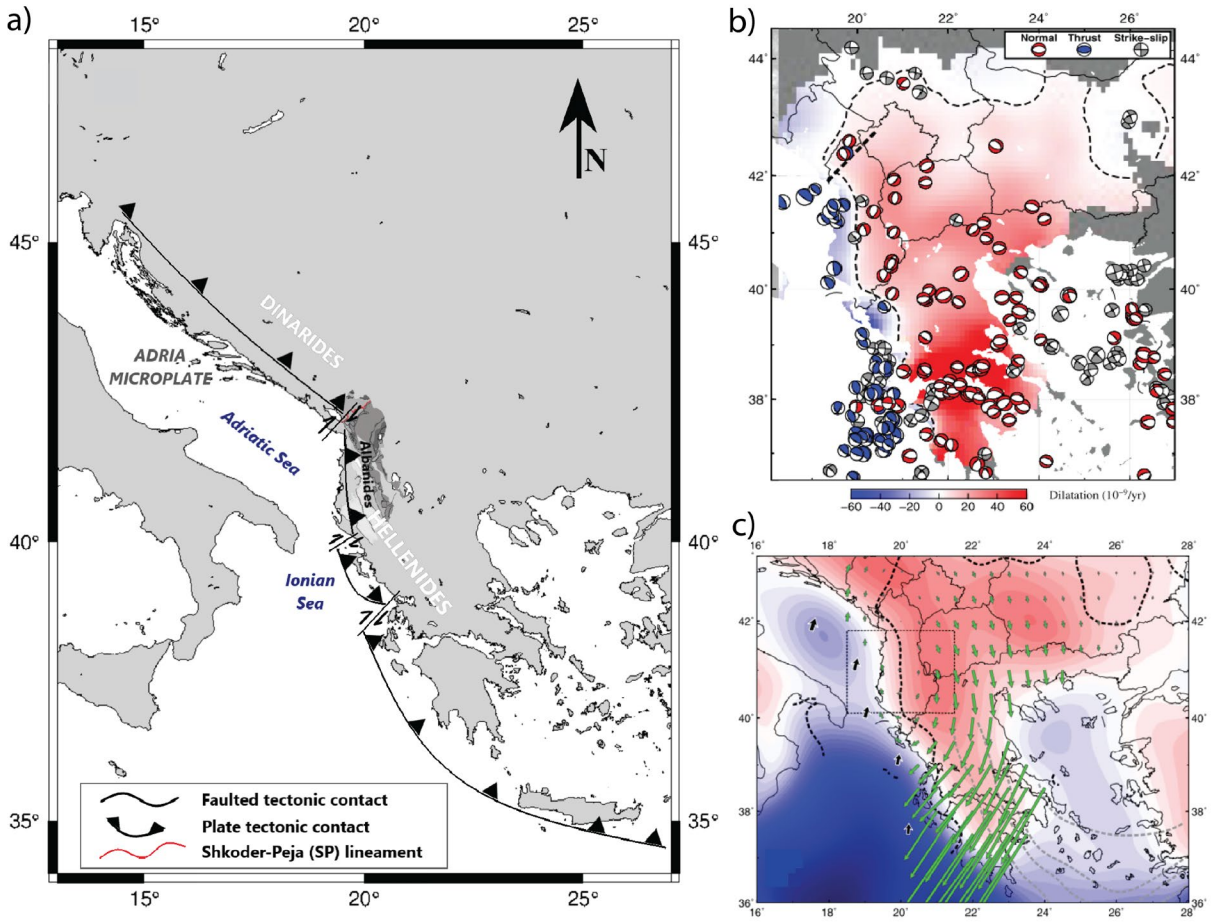

Figure 2. a) Regional tectonic scheme of Dinarides-Albanides-Hellenides, part of the Euro-Mediterranean Alpine belt, with indication of the main tectonic contacts; b) Dilatational strain and focal mechanisms from GCMT database [http://www.globalcmt.org), for the time span 1976-2019, depth ≤25 km and Mw ≥5.0 and c) Interpolated regional GPS velocities relative to Eurasia (b and c modified from D'Agostino et al. [2020]).

Hellenic folded orogenic structure [Mihaljevic et al. 2017]. Along the Albanian coastal region the orogenic front is thrusting over the Adria microplate, partly over the Apulian platform and partly over the Southern Adriatic Basin [Aliaj 2006]. The segment of the orogen in Albania is sometimes referred to as the Albanides [Meço et al. 2000; Handy et al. 2019]. According to Aliaj [2006] and Jouanne et al. [2012], the orogen in Albania includes two tectonic domains, differing by their present-day stress regime, respectively: the outer westernmost domain, dominated by shortening and compression and the inner one, under multidirectional extension. In Albania, the Adria-orogen collision takes place along the outer tectonic domain. According to D'Agostino et al. [2020], the separation between these two domains follows remarkably a zero dilatation contour (dashed line, Figure 2b and c), characterised on each side by reverse and normal focal mechanisms respectively (Figure 2b). At the transition zone, between positive and negative dilatation regions, strike-slip earthquakes occur [D'Agostino et al. 2020]. Based on the focal mechanism of shallow earthquakes (Figure 2b), from the GCMT catalogue [Ekström et al. 2012], and many other studies [Muço 1994; Aliaj 2006; Mihaljevic et al. 2017; Dushi et al. 2018; D'Agostino et al. 2020], the horizontal compression dominates along the Adriatic collision, while extension dominates in the internal domain.

According to Jouanne et al. [2012], the velocity field obtained from permanent and/or episodic GPS stations in Albania and surroundings (Figure 2c), is characterized by southwestward motion of outer Albanides and southward motion of inner Albanides, increasing both from north to south. The Albanides structure undergoes a clockwise rotation indipendently from any reference frame [D'Agostino et al. 2020]. In the outer region the system of assumed active faults are almost linear (Figure 3), trending SE-NW. In the inner part of the territory, due to the extensional tectonic regime, normal faulting dissects and cuts through the area, with some rarely observed overthrusts [Jouanne et al. 2012]. In contrast to the outer domain, the orientation of faults in the inner one, has a N-S direction.

The Adriatic collision zone is the most seismically active zone in Albania, which is represented by the Ionian-Adriatic coastal earthquake belt (Figure 3), along the eastern margin of the Adria microplate [Aliaj 2006].

4. Seismicity

The seismicity of Albania is moderate and is mainly characterised by small and medium-sized earthquakes, and rarely by large ones [Muço 1995]. Figure 3 shows the seismicity of Albania using data from the International Seismological Center (ISC) for the period 1980-2020 [Lentas et al. 2019; Storchak et al. 2020]. Events are restricted to be located by a minimum of 20 stations, have less than 10 km error in any direction and minimum magnitude of 4.0. There are 1066 events selected and 23 are below 40 km depth. So, the majority of earthquakes in Albania are crustal although we see a weekly developed subduction zone. This observation is in good accordance with the previous results on seismicity studies in Albania. According to Muço [1995], the seismicity of Albania is mostly shallow, exceeding 50 km of depth only in few cases. Later, applying a new crustal velocity model [Ormeni 2009], it was revealed that most of the seismicity was confined within the upper crust, although deep crustal and sub-crustal seismicity is noted as well, mainly in Western and Southern Albania. For earthquake location, it is then the crustal 1D structure above Moho, as well as the Moho velocity, which is the most important.

It is seen that the seismic activity is mostly concentrated in western and eastern part of our study area where we also find most of the geological faults.

5. Crustal models published for Albania

The published and documented velocity models for Albania are described in the following, see Table 1 and Figure 6. Two velocity models were used with the old programs of the analogue data period [Muço 1998; 1999], based on a single and a two layered structure. The single layer model had a crustal thickness of 40 km and a linearly increasing P-velocity. Peçi and Shubleka [2001] proposed a model based on 16,009 earthquakes. Data used for this crustal model were distributed within the area 39°-43°N and 18.5°-21.5°E and using seismic stations as far as 900 km away. The velocity models, given in Table 1 and Figure 6 for these 2 studies, are linear increasing step models discretised for each 5 km depth.

Muço et al. [2002] provided a comprehensive overview of the knowledge until 2000 and also proposed two new models, Model 1 for the western tectonic domain and Model 2 for the eastern part. It is well known [e.g., Halpaap et al. 2018; Dellong et al. 2018] that the crustal thickness increases from the sea to the interior of Albania and the

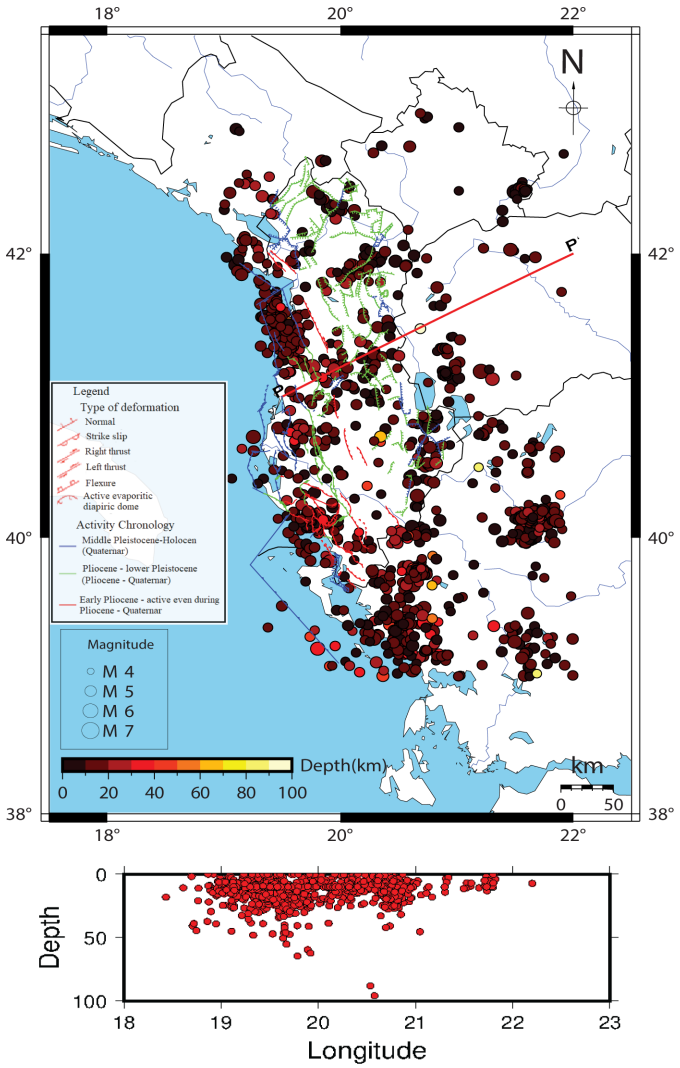

Figure 3. Top: ISC seismicity for 1980-2020 and known geological faults of Albania. Bottom: Depth profile of projected earthquakes along the red line (P:40.99N;19.50E, P′:42.0N;22.0E), including 1055 of 1066 events (area 600 × 500 km), seen on the map. Data is taken from the International Seismological Centre [2021], On-line Bulletin, https://doi.org/10.31905/D808B830.

biggest difference between the two models is the Moho depth. In Model 1 it is 30 km and in Model 2 it is 40 km. The abrupt change of Moho from 30 to 40 km is of course not realistic, but a way of describing the change in Moho depth. It is seen that the two models are very similar with the main difference being the extra layer of 7 km/s and the deeper Moho in Model 2.

Ormeni [2011] made a study of the crust using the VELEST program [Kissling et al. 1995]. This model has 23 layers which seems unrealistically detailed. Ormeni also made an average model with Moho at 50 km. This seems too deep for an average model (see later) but might be correct for the eastern part.

For the last 10 years the model shown (current model) in Table 1 has been used for routine earthquake locations. It is seen that the current model is the Ormeni model without the layer starting at 55 km. A sub-Moho velocity of 7.6 km/sec seems a bit low, but most studies referenced here, seem to indicate this to be correct.

Based on tomographic inversion, the structure along the Western Hellenic Subduction Zone south of Albania was determined by Halpaap et al. [2018] (Figure 4). The average velocities are given in Table 1 based on a detailed table given by Halpaap [personal communication, 2020]. This average model was calculated for the area between 5 and 95 km from the coast. The Moho depth is between 40 and 50 km (average 45 km) and the Moho velocity around 7.6 km/sec. The Moho in the western part is deeper than in the European Moho model, but then the Halpaap study is based on additional data. V_p/V_s is determined to be 1.78 to 1.82. The Halpaap model is close to the Ormeni models, except for V_p/V_s.

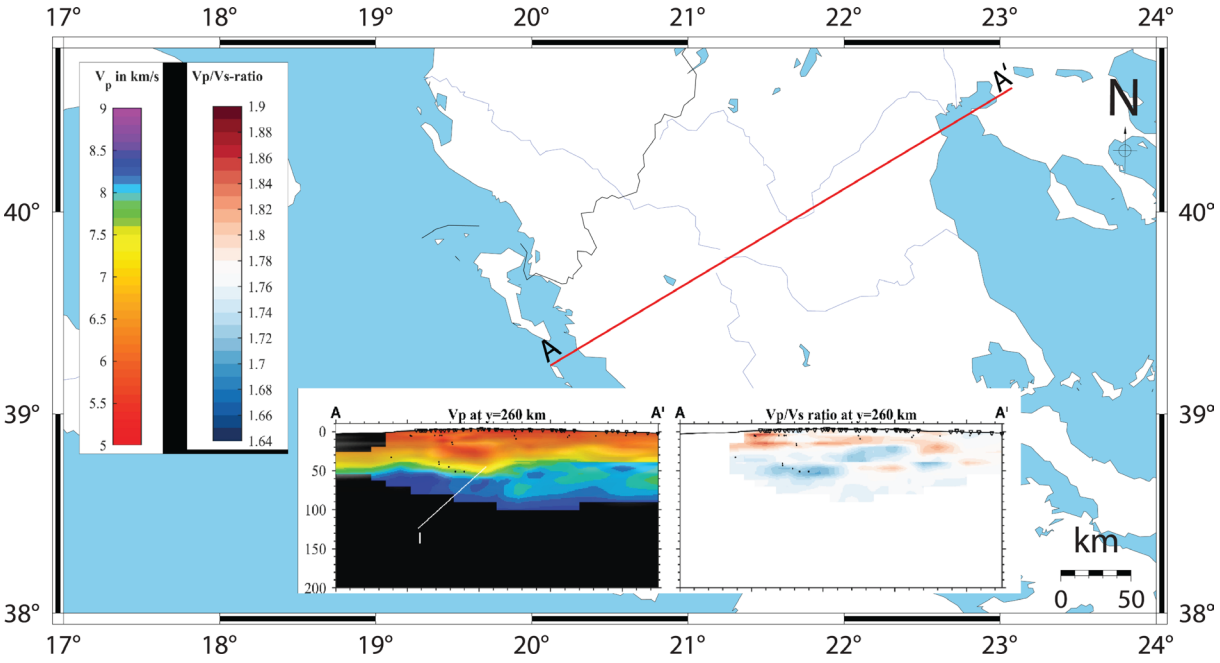

Figure 4. Model from Halpaap et al. [2018]. Profile A-A′ goes through southern the Albania-Greece border region.

Obviously, as seen from the Halpaap model, the crust of Albania is more complex than a simple 1D model and a few previous studies have also suggested a more complex structure. Ormeni [2009] calculated crustal models for different area of Albania using VELEST. He found regional differences as well as some evidence for low velocity zones. This work was expanded to make a 3D tomography study confirming the existence of significant regional

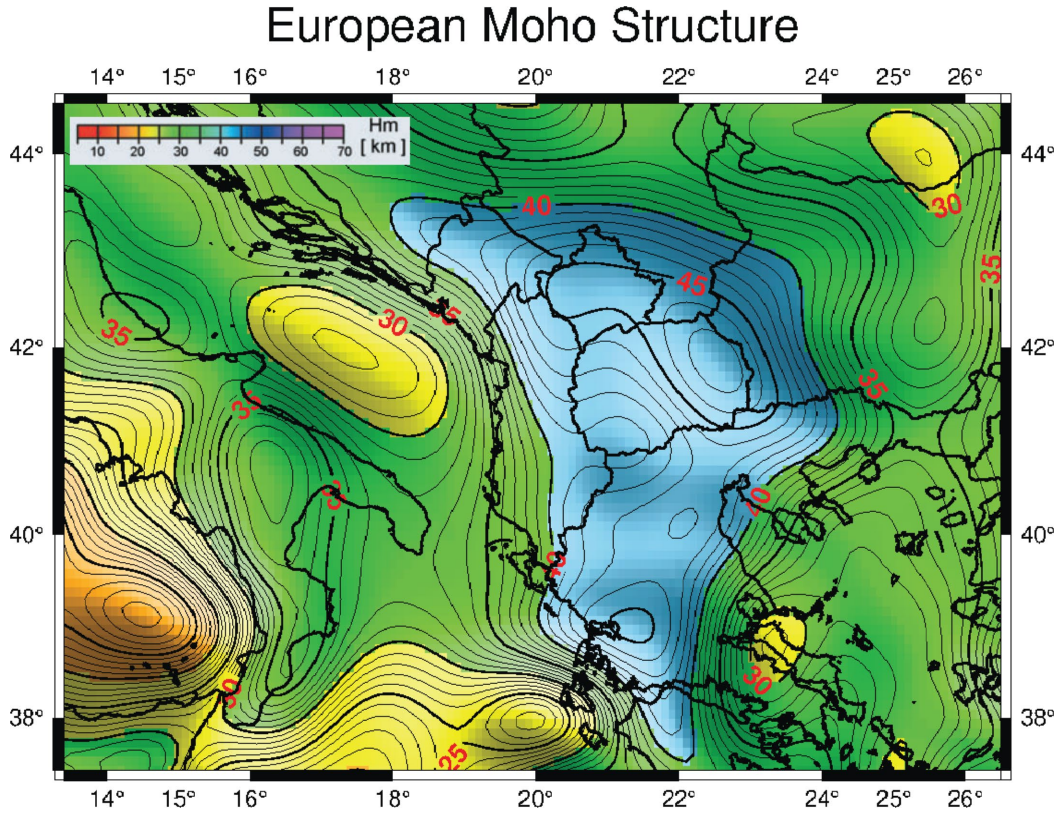

Figure 5. Moho map of the Adria and Albania region, taken from Grad et al. 2009. https://www.seismo.helsinki.fi/mohomap.

velocity variations as well as low velocity zones. Papazachos et al. [2002] also, presented results from tomographic studies, indicating similar regional variation.

Several studies have proposed Moho depths for Albania and surroundings. The regional section based on the open data of the European Moho Map, is plotted in Figure 5 [Grad et al. 2009]. It is seen that Moho is estimated to be between 35 km to the west and 45 km to the north east.

A Moho depth of around 45 km for a region partly including the eastern Albanian border region, was determined by Delipetrov et al. [2016]. Although there are no direct measurements in NNW Albania, the Moho depth in this part seems to be around 40 km, based on the Moho depth study for Croatia and N. Adriatic Sea region [Stipčević et al. 2011], which is deeper than that given by the European Moho Map (Figure 5). Dellong et al. [2018] found a Moho depth of 18 km (Vp = 8.1 km/s) out at sea (38N, 19E), which corresponds to an oceanic crust within the Ionian basin (Central Mediterranean Basin) along a transform margin of Malta escarpment. This shows that the crust is considerably thinner offshore to the most southwestern border of Eurasia plate [Dellong et al. 2018].

6. A new preliminary start model

The most recent and detailed model is the Halpaap model, although it is a bit at the extreme south end of our study area. It has some similarities with the Ormeni model and we will base the start model on the Halpaap model with some consideration of the Ormeni model. The earlier Muço and Peçi models deviate significantly from both Ormeni and Halpaap.

Different velocity models for Albania																
Depth (km)	Muço [1998;1999]			Ormeni [2011]		Current		Peçi& Shubleka [2001]		Muço-1 [2002]		Muço-2 [2002]		Halpaap [2017]		Start	
	N of 41°/S of 41°			V_P (km/sec)													
0	5.5	5.2		5.2		5.1		5.0		4.4		4.4		5.8		5.7	
5	5.5	5.3		5.8		5.8		5.7		5.9		4.8		6.1			
10	5.6	5.4		5.9		5.9		5.9		5.9		6.0		6.0		6.2	
15	5.7	5.4		6.0		6.1		6.2		5.9		6.0		6.2			
20	5.8	5.5		6.3		6.3		6.5		6.0		6.0		6.1			
25	5.9	5.6		6.3		6.3		6.9		6.0		7.0		6.2			
30	6.0	5.7		6.5		6.5		7.1		**8.0**	M	7.0		6.5		6.7	
35	6.1	5.8		6.7						8.0		7.0		6.8			
40	6.2	5.8		7.1		7.1		**7.9**	M	8.0		**8.0**	M	7.2		**7.6**	M
45	**8.2**	**8.2**	M	7.4				8.1		8.0		8.0		**7.6**	M		
50	8.2	8.2		**7.6**	M	**7.6**	M			8.0		8.0					
55	8.3	8.3		7.9										8.1			
60	8.3	8.3		8.1										8.3			
70	8.5	8.5												8.3		8.2	
V_p/V_s				1.71-1.78		1.74		1.74		1.73-1.80		1.75-1.86		1.78-1.81		1.80	

Table 1. Comparison of different models. Most models used boundaries every 5 km so to make the comparison easy, only 5 km boundaries have been used. If no data is given at the 5 km boundaries, they have been estimated. "Start" is our proposed start model, "Current", is the currently used model and M is Moho.

From the previous publications, it seems that an average Moho depth of 40 km should be used in the study area, and it seems that Moho is not as shallow as 30 km in the western part. This is of course too high for offshore but most events are located onshore or near onshore. Many authors agree that the Moho velocity is around 7.6 km/s [Ormeni 2011; Halpaap et al. 2018].

There is not a lot of reliable information on where the different interfaces are located so it seems better to make a simplified model with only a few layers. Ormeni made an average 3-layer model above Moho meant for earthquake locations so we will also try a three-layer model. The start V_p/V_s ratio will be based on Halpaap since that study had the most recent and detailed data set. The comparison between all the mentioned models and our proposed start model is seen in Table 1 and Figure 6. It is seen there is quite a large variation between the models which have been used.

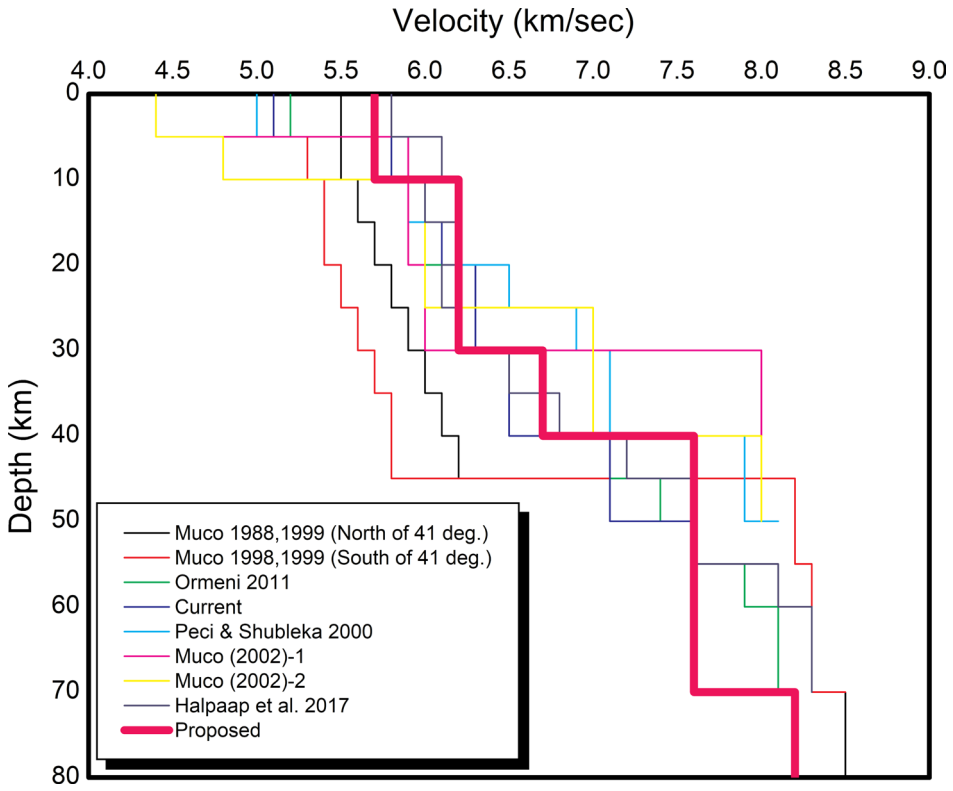

Figure 6. Comparison of velocity models for Albania as given in Table 1. Proposed is our proposed start model.

7. Data

The overall goal was to use the most reliable earthquakes with uniform coverage of the country. The following selection criteria was used for the initial event search:

- At the time of starting this work, it was not known what waveform data was available. However, the original phase readings and locations had been recovered. The potential events were therefore selected using this data base under the assumption that if phase readings were available, the waveform data was also potentially available. This limits the data to the period 2008-2020.
- Only events recorded at stations in Albania or near Albania were used to make the model representative of the local area.
- Events located by ISC, with more than 20 stations, depth > 15 km and location error less than 10 km in any direction (127 events), in order to have reference events.
- Local events with more than 8 local stations, 66 events.
- Some additional local events to fill spatial gaps, 7 events.

This gave a list of 200 potential events. When searching the old data, little waveform data was available before 2012 and the available data set ended up with 108 events (Figure 7).

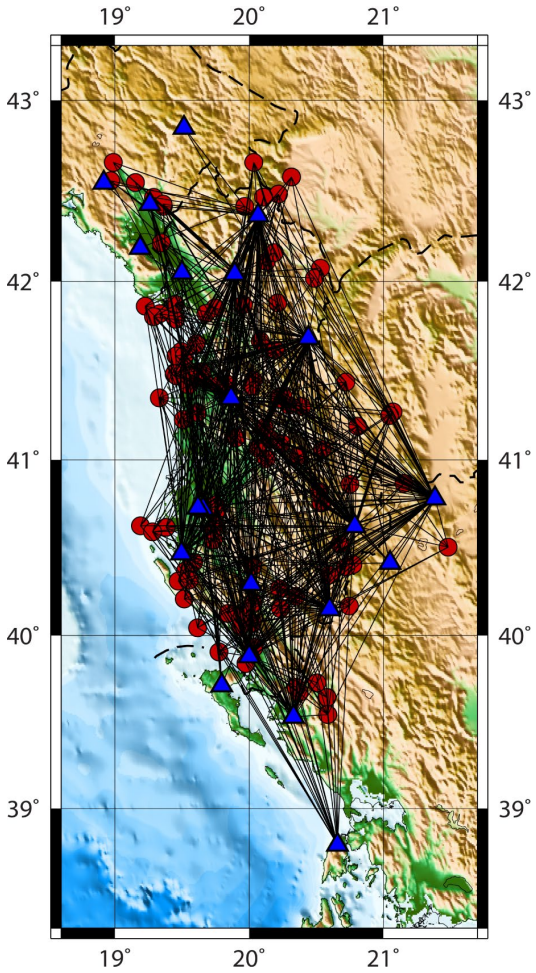

Figure 7. Data used. The red circles are epicenters the blue triangles the stations and all P and S rays are shown.

8. Data processing

All phases was re-read to obtain higher quality data. A particular problem is reading S-phases. For near stations (up to 100-130 km depending on depth), the S-phases were mostly clear and assumed to be first arrivals. S-phases up to 100 km distance were usually given full weight. For distances 100 to 250 km, S was given weight 0.5 or 0.25 depending on the quality. For distance further then 100 km, many P-phases were small and emergent indicating refracted phases so the large S-phases were often labeled Sg assuming that the refracted S-phase could not be seen. In cases where P was clear and relatively large, the S-phase was labeled S to indicate first arrival. For relocation, a distance weight was used with full weight at 150 km and zero weight at 250 km due to the uncertainty of phase interpretations at larger distances and the possibility of lateral velocity variations and to make sure the data were representative for the local area. All data were also checked with Wadati diagrams [see e.g. Havskov & Ottemöller, 2010] to make sure there were no large errors. The initial locations and checks were made with the new start model. Depths were in the range 0 to 85 km with 5 events below Moho (Figure 8), and these events are probably related to the subduction zone. The average depth was 20 km.

It is well known that the crustal thickness is much less in the Adriatic Sea than inland Albania (as discussed above) so in order to not bias the data, no stations from Italy were used although they fulfilled the distance range condition.

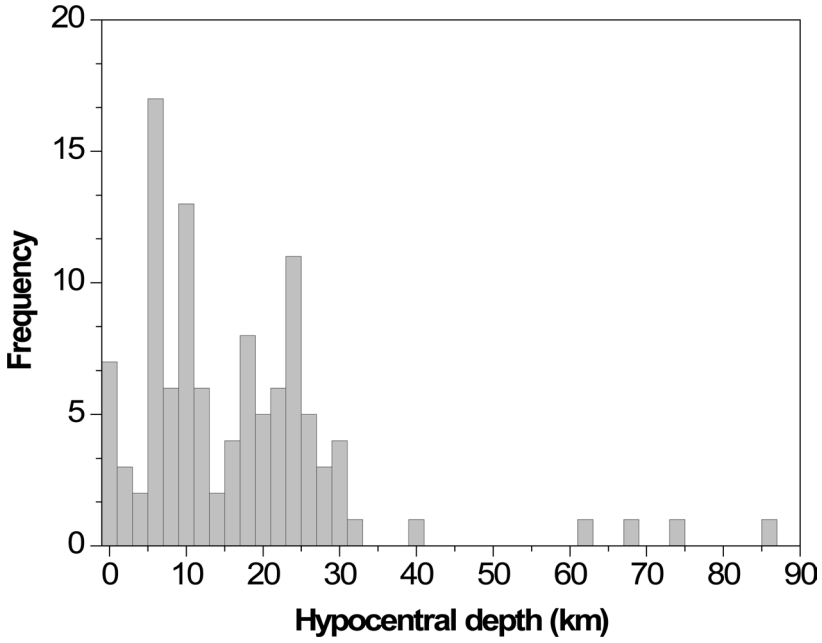

Figure 8. Hypocentral depth frequency distribution.

9. Grid search for a new model

The 108 events were relocated using models varied in a systematic way. We assumed a constant velocity below Moho since our data only had one event which potentially could be located below the possible layer of 70 km. The model space was systematically searched for the 30 models giving the lowest average RMS of travel time residuals. Typically, at least 10,000 models were used in each test. Both P-velocities, layer thickness and V_p/V_s were varied in the same run, but not V_P and V_S independently since this would give too many models to check. The grid search is done by varying each parameter in turn and keeping the others constant so each model in the range specified is used. So, if e.g. 10 different velocities are used for the first layer, 10 for the second, 10 different layer thickness for first layer and 10 for the second layer, a total 10,000 models are tested. For each test, the 30 models with the lowest RMS are kept in order to get an idea of the variation of the best solutions since in all tests, the various parameters play off against each other like increasing the velocity in one layer and decreasing in another might give similar RMS as doing the opposite. This is described in more details in the practical tests below. The location program used was Hypocenter [Lienert et al. 1986, 1995] as implemented in SEISAN [Havskov et al. 2000; Havskov et al., 2020].

An alternative way to determine the crustal structure is to use VELEST [Kissling et al. 1995]. Using VELEST, a whole data set of first arrival phases from many events is inverted for layer velocities and hypocenters while the layer thickness is kept constant so a grid search will also have to be done for layer thickness and V_p/V_S. Since VELEST only uses first arrivals, this would severely limit our data set and doing grid search is a simple alternative where all data can be used.

9.1 Test with synthetic data

Our grid search is a simple brute force method and in order to test how well it works, we first tested with synthetic data. Using the test model seen in Table 2, synthetic arrival times were calculated for the 108 events using the same phases and the same weights as in the original data and the grid search done with different levels of noise. The V_p/V_s was fixed at 1.81 which is later found to be the best value.

First, the test was done with no noise and not surprisingly, the start model was recovered exactly. Then uniformly distributed noise was added to the data, $\pm$ 0.5 s and $\pm$ 0.9 s for P and S respectively in the first test and $\pm$ 1.0 s and $\pm$ 1.8 s for P and S, respectively in the second test. The noise was independent for P and S.

Test model	L2	L3	L4	V1	V2	V3	V4	RMS [sec]	Nmod	MRMS
	10 [km]	20 [km]	40 [km]	5.0 [km/s]	6.0 [km/s]	7.0 [km/s]	8.0 [km/s]			
Initial test with noise = ± 0.5 s										
Range	6-12	13-25	32-44	4.6-5.5	5.6-6.5	6.6-7.5	7.6-8.5		43200	0.846
Step	3	3	3	0.3	0.3	0.3	0.3			
Best	12	19	38	4.9	6.2	6.9	7.9	0.327		
R30	9-12	19-25	32-44	4.9-4.9	5.9-6.2	6.9-7.2	7.6-8.2	0.345		
AV	11.8	21.2	39.2	4.9	6.2	7.0	7.8			
SD	0.8	2.3	3.9	0.0	0.1	0.2	0.2			
Initial test with noise ± 1 sec, with same parameters as above for noise = ± 0.5 s										
Best	12	19	32	4.9	6.2	6.9	7.6	0.598	43200	1.017
R30	9-12	19-25	32-44	4.9-4.9	6.2-6.2	6.9-7.2	7.6-8.2	0.609		
AV	11.8	21.2	39.2	4.9	6.2	7.0	7.8			
SD	0.8	2.2	3.9	0.0	0.1	0.2	0.2			
Final test with ± 1 sec										
Range	6-12	18-22	37-46	4.8-5.1	5.8-6.2	6.8-7.2	7.8-8.4		11520	0.768
Step	2	2	3	0.1	0.1	0.2	0.2			
Best	12	20	40	5.0	6.2	7.0	8.0	0.583		
R30	10-12	18-22	37-46	5.0-5.0	6.1-6.2	6.8-7.0	7.8-8.2	0.588		
AV	10.8	19.7	40.8	5.0	6.1	7.0	8.0			
SD	0.6	1.3	3.3	0.0	0.1	0.1	0.2			

Table 2. Model space searched in the ranges indicated in the table. Abbreviations: Lx: Depth to interface x (km), Vx: velocity in layer x (km/s), RMS: Average RMS(s) for the best model or 30 best models, MRMS: model with maximum average RMS(s) for test, Test model: Test model, Range: Range of parameters, Step: steps in grid, R30: range of models among the 30 best, Best: model with lowest average RMS(s), AV and SD: average and standard deviation of the 30 best models and Nmod: number of models tested.

In the first test, quite a large model space was searched as also seen by the maximum average RMS. Based on the 30 best models, smaller and smaller ranges were used. Only the initial test for 0.5 s and 1.0 s noise and the final test for 1.0 s noise, are shown. The 30 best models have nearly the same RMS so the variation between them gives an indication of the uncertainty of the model determination. In order to give an indication of the spread of models with similar RMS, the average parameters were also calculated for the best 30 models. Summary results of the tests are seen in Table 2.

Both tests with different noise levels result in nearly the same average minimum RMS model. The tests also show that several similar models give almost the same RMS so the parameters will play off again each other as seen with the range of models within the best 30 models. The uncertainty is more pronounced for layer thickness than for velocities. However, for the ranges tested, there is clearly a group of models with similar minimum RMS. One can argue that we already know the correct model so searching around that naturally gives the correct results. However, the data space searched was quite large so we feel confident that we really find the minimum model. The layer thickness was obtained within 0-2 km of the test model and velocities within 0-0.2 km/s of the test model. Clearly the inclusion of noise systematically gives a different model than the test model. We have not investigated if other noise distributions might have given a different result like e.g. not using that noise in the S data as V_p/V_s times the noise is the P arrivals. The noise in S could be different from what we use but generally the S is more

uncertain than the P. Note that the test with highest noise level gives an RMS similar to the RMS in our real data, see Table 4.

9.2 Search for a new model using the 108 events

First it was investigated how the data samples the start model. Locating with the start model the phases in different layers are counted, see Table 3.

Phase	Direct	Refracted		P_n/S_n
	G	N2	N3	N4
#P	387	184	9	117
#S	535	80	2	77
W_P	334	135	6	39
W_S	330	45	1	14

Table 3. Number of different phases using the test model. G is Pg or Sg, N2-N4 are refracted phases at interface 2-4 so N4 is the Pn/Sn phase. #P and #S is number of phases and W_P and W_S is the sum of the weights used for P and S respectively.

It is seen that the largest number of phases used are Pg and Sg (922 phases) while there are only 194 Pn and Sn phases and 275 other refracted phases so about twice as many direct phases as refracted phases. So, the direct phases dominate in the grid search. This domination of direct phases is even stronger than these numbers indicate since many phase weights are smaller than 1.0 due to distance weighting and weighting down uncertain S-phases. The total number of phase weights for Pg and Sg is 664, for Pn and Sn 53 and for other refracted phases 180, so the total weight of direct phases is almost 3 times the total weight of direct phases. The interface with the fewest refracted phases is the third interface so we can expect it to be the least well determined.

The grid search was done as outlined with the synthetic data with finer and finer grid as the final model converged. V_p/V_s was also varied in the range 1.70 to 1.85 but it soon became clear that V_p/V_s always were in the range 1.80 to 1.82 with the best fitting value of 1.81 so V_p/V_s was kept at 1.81 in most tests.

In order to evaluate the results, one should look for models with the minimum average RMS in the model space. The question is if there are other significantly different models with almost the same RMS. Looking at the 30 best models as well as their average gives an indication as discussed under tests with synthetic data. We also tried to take the average of more than the best 30 models but it gave little change in the average model for the first few hundred best models. The results are seen in Table 4. The table only shows the first and the last test.

The interfaces, except the third, seem to be determined with an error of about 1 km and the velocities with an error of 0.1 km/s. The velocities seem stable with the average close to the best value and with a small standard deviation. However, it is clear that all parameters play off against each other within a small RMS variation so all 30 models would be equally good. This shows that there is no point in trying to use a model with more layers. The range of depths to interfaces for the 30 best models, show the largest variation for interface 3, as expected considering the few refracted phases from that interface. We will choose the model with lowest RMS which in all cases also is within 0.1 km/s in velocity and 1 km in layer depth of the average of the 30 best models except for depth to interface 3. For this interface we set that for the final model, the variation of layer depth for the best 30 models is 5 km while for the other 2 layers is between 0 and 2 km. So, interface 3 is clearly the least well determined.

Since the phases were picked using the start model, there is a potential for picking phases, particular for S, that fit that model and therefore bias the results. The grid search was therefore also done with P-phases alone (Table 4). Locating only with P gives less reliable solutions and 4 events could not be located. So, this gives less well constrained solutions but gives an indication of the accuracy of the results. The velocities obtained are similar to the velocities for the models using P and S. The first interface moves from 12 to 8 km and the second from 23 to 31 km,

Start	L2	L3	L4	V1	V2	V3	V4	RMS	Nmod	MRMS
	10 [km]	30 [km]	40 [km]	5.7 [km/s]	6.2 [km/s]	6.7 [km/s]	7.6 [km/s]	0.557		
First test										
Range	8-14	16-36	36-42	5.2-5.8	5-9-6.3	6.4-7.0	7.2-8.2		27648	
Step	2	4	2	0.2	0.2	0.2	0.2			
Best	12	24	40	5.4	6.1	6.4	7.6	0.497		0.915
R30	8-14	24-36	38-42	5.4-5.6	5.9-6.1	6.4-7.0	7.4-7.8	0.500		
AV	12.3	31.6	40.6	5.6	6.1	6.6	7.7			
SD	1.3	4.3	1.3	0.1	0.1	0.2	0.1			
Final test										
Range	10-13	22-28	39-44	5.4-5.6	5.9-6.2	6.3-6.7	7.5-7.9		50400	
Step	1	1	1	0.1	0.1	0.1	0.1			
Best	12	23	41	5.5	6.0	6.3	7.7	0.490		0.609
R30	12-12	23-28	40-42	5.5-5.6	6.0-6.0	6.3-6.5	7.6-7.8	0.493		
AV	12.0	24.7	41.3	5.5	6.0	6.4	7.7			
SD	0.0	1.5	1.2	0.0	0.0	0.1	0.1			
Final test with P only										
Range	7-11	30-35	37-42	5.4-5.6	5.8-6.2	6.3-6.7	7.5-7.9		67500	
step	1	1	1	0.1	0.1	0.1	0.1			
Best	8	31	42	5.5	6.0	6.7	7.9	0.256		0.320
R30	7-9	30-33	37-42	5.4-5.5	5.9-6.0	6.3-6.7	7.6-7.9	0.258		
AV	7.8	31.1	40.7	5.5	6.0	6.6	7.8			
SD	0.6	1.2	1.6	0.1	0.0	0.1	0.2			

Table 4. Model space searched in the ranges indicated in the table. Abbreviations: Lx: Depth to interface x (km), Vx: velocity in layer x (km/s), RMS: Average RMS(s) for the best model or 30 best models, MRMS: model with maximum average RMS(s) for test, Start: Start model, Range: Range of parameters, Step: steps in grid, R30: range of models among the 30 best, Best: model with lowest average RMS(s), AV and SD: average and standard deviation of the 30 best models and Nmod: number of models tested.

while the Moho depth only moves from 41 to 42 km. This difference could indicate that S is not picked correctly, which could be due to the onset of S being masked or distorted, by the P-wave coda. The result also indicate that location of particularly the third interface is quite uncertain.

We will use the model with the best results from the P and S data since this represent the data actually used for locating earthquakes and is also the data giving the most reliable hypocenters. Ideally only clear P-arrivals should be used, but this requires a much denser network than currently available.

9.3 Residuals

Table 5 shows the average residuals with standard deviation for stations with more than 5 P-phase readings. It is seen that the average residuals for P and S residuals are small with standard deviation typically around 0.4-0.8 s. This indicates that the travel times, used with this data set, do not seem to be systematically affected by the structure. However, the relatively large standard deviation indicates some uncertainty in the arrival times.

Station	AV P	SD	no P	AV S	SD	no S
BCI	0.04	0.76	67	–0.08	0.52	65
BPA1	0.32	0.61	14	0.01	0.27	16
BPA2	0.13	0.56	14	0.15	0.35	13
FNA	0.07	0.56	69	–0.35	0.55	62
IGT	0.01	0.78	46	–0.28	0.88	42
KBN	0.06	0.56	57	0.11	0.53	62
LKD2	0.13	0.59	31	0.47	0.42	23
LSK	–0.12	0.53	43	0.15	0.46	42
NEST	–0.04	0.51	10	0.03	0.49	9
PHP	–0.18	0.45	74	0.13	0.46	71
PUK	0.01	0.43	56	0.03	0.43	52
SRN	–0.03	0.51	55	–0.15	0.54	56
TIR	–0.03	0.37	75	0.12	0.45	77
TPE	0.10	0.52	9	0.31	0.50	8
VLO	0.18	0.57	39	0.43	0.50	40
PDG	–0.30	0.29	7	–0.12	0.67	8

Table 5. Average P and S residuals with standard deviation for stations with more than 5 readings. Abbreviations: AV P: Average of P residuals(s), SD: Standard deviation(s), no P: Number P readings, AV S: Average of S-residuals(s), no S: Number of S-residuals.

9.4 Comparison with ISC and original locations

Since we have no ground truth events it is difficult to evaluate if the locations are more accurate than before. For 62 of the events, there are ISC hypocenters located with at least 20 stations and estimated location errors less than 10 km in any directions. Table 6 compares the ISC locations of earthquakes (magnitude range Mb 3.6 to 5.0) to the locations of the original hypocenters and to the hypocenters located with the final model and the newly picked data. It is seen that the average difference in location for the two data sets are quite similar but the standard deviation in the location and origin time differences are about twice as large for the original data as for the new data indicating that the overall location accuracy has been improved. This is maybe partly also because of a more carefully picked phases in the test data set. We therefore also relocated the events with the new readings using the current model and also in this case is the difference with ISC locations larger than using the new model.

	Origin time	Latitude	Longitude	Depth
ISC compared to new locations SD	0.8 0.9	–0.005 0.035	–0.039 0.058	–0.9 7.8
ISC compared to original locations SD	1.6 3.9	–0.012 0.089	0.024 0.127	3.2 13.0
ISC compared to locations with original model SD	1.1 1.2	–0.011 0.058	–0.001 0.104	0.3 12.2

Table 6. Comparing locations and origin times to corresponding ISC locations. The columns show, for 62 events, average difference in origin time(s), location(degrees) and depth(km). SD is standard deviation.

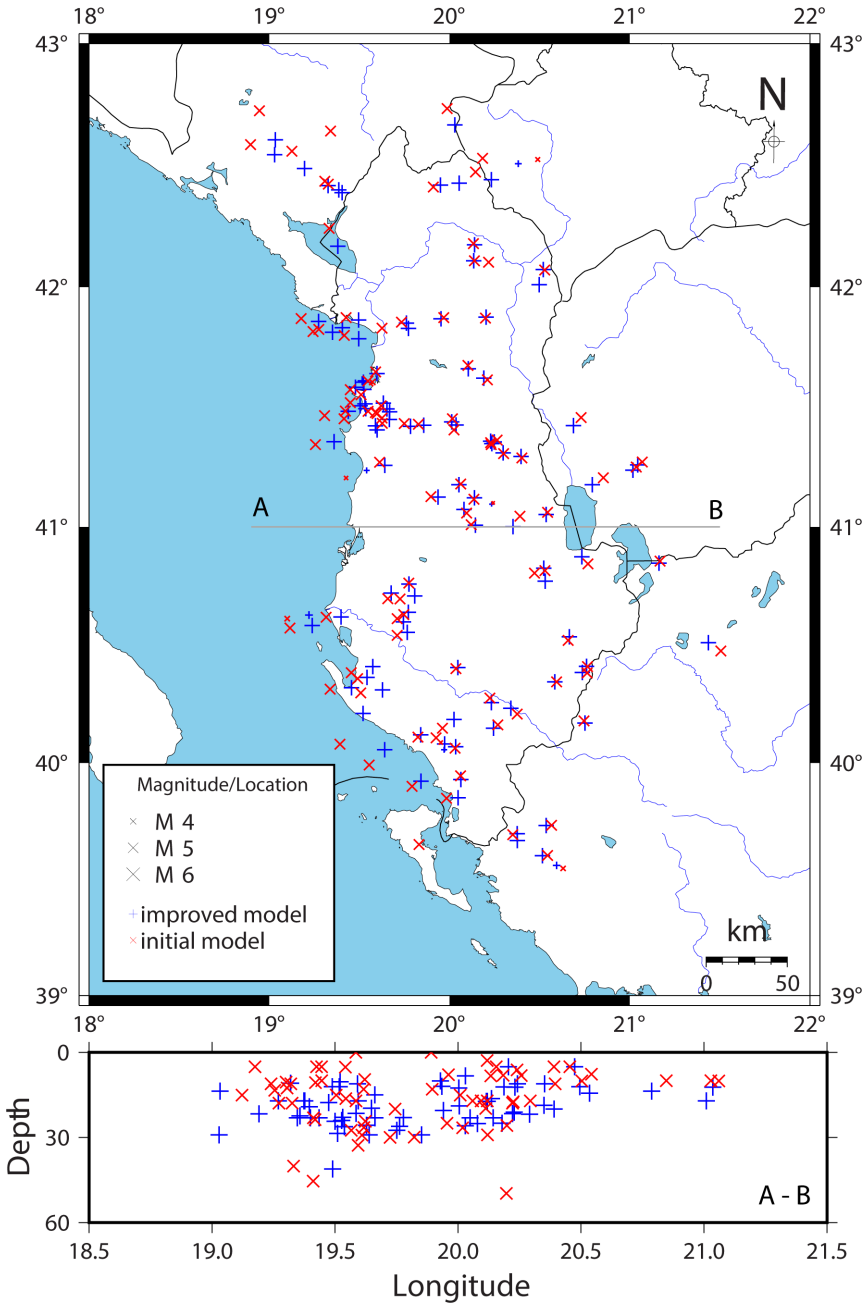

Figure 9. On top is seen the epicenters located with the original model (red) and the final model (blue). On the bottom is shown a depth profile from West to East.

We have also compared the locations done with the original model and the new model, see Figure 9.

It is seen that inside the network there are little epicenter change while on the outside there are larger changes. This is what should be expected. The depth distribution of events show that there are fewer events below Moho with the new model than with the old model. With the new model the events are less spread out in depth and there is only one event with the unrealistic depth of 0 km while with the original model there were 7 events.

10. Discussion and conclusion

The model determined seems to represent a well-defined minimum and the grid search seems to work well as also demonstrated with the synthetic data. Many similar models give almost the same average RMS and the average parameters for the 30 models with the lowest RMS have a variation of up to $\pm$ 1.5 km in layer thickness and up

to ± 0.1 km/s in velocity. The final model is compared to the currently used model and the start model as seen in Figure 10 and Table 7.

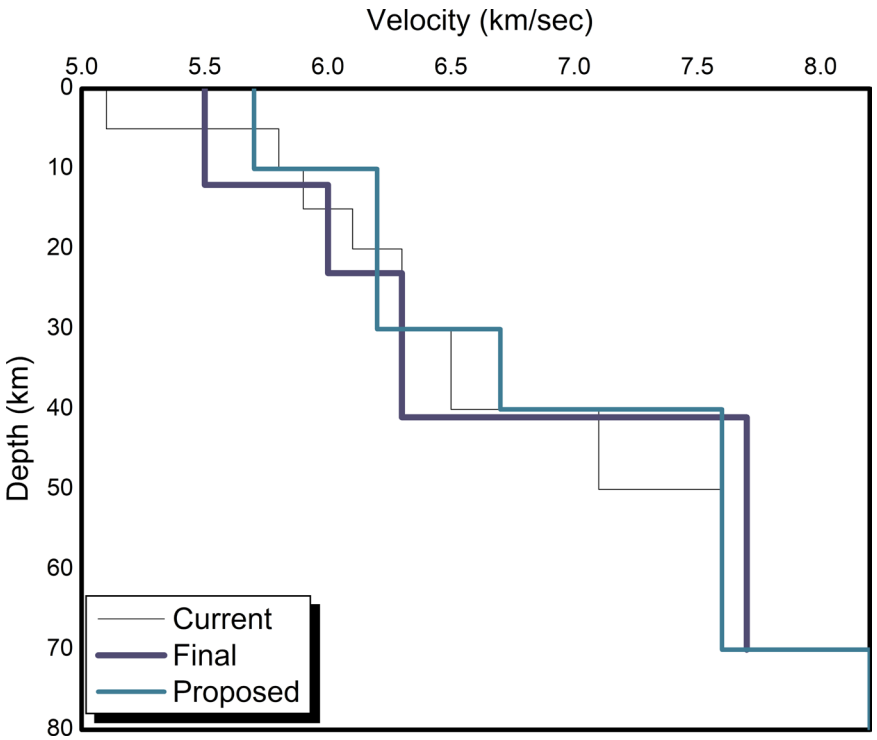

Figure 10. The proposed start model, the currently used model and the final model.

It is seen that the final model is close to the current model until 30 km depth, then it has lower velocity then both start and current models until 40 km and is finally close to the start model below 41 km.

The S-phases were the most uncertain to read and it is not always easy to judge if an S-phase is Sg or a refracted first arrival and this could bias the solution. Using only P-phases for the grid search gave a somewhat different model where particularly the layer thickness was different by a few km. Ideally only clear P-phases should be used to avoid an ambiguity in S-phase identification. However, in practice this is mostly not possible since, for small networks, like the Albanian network, the S-phases are needed to get a reliable solution. In general, it is seen that both when using P and S and P only, the layer thickness is the most unstable parameter, particularly for interface 3, while the velocities determined seem very stable. This shows that using a model with more layers is not realistic and that the current data is not able to reliably resolve the position of the third interface.

Despite the varying tectonics across Albania, we do not see any obvious correlation with the average station residuals and we conclude that the model, with the accuracy of the data, is not able to detect the varying tectonics. The final model used will be the one based on both P and S since this is what is used in practice. The final model is different from both the start model and the current model and we conclude that the average Moho depth is close to 41 km as also indicated in some of the latest studies, e.g. Halpaap et al. [2018]. The new locations are now closer to the ISC solutions than before and the average RMS has been reduced significantly. We conclude that we have obtained a new crustal model for Albania and close surroundings which is a significant improvement on the previous model used for location. This does not mean that this is the most correct model, but it is the model giving the lowest RMS when locating earthquakes with a 1D model.

Data and sharing resources. The data underlying this article is available at www.geo.uib.no/seismo/REPORTS/ALBANIA-CRUST/ and the software used is found at seisan.info.

Acknowledgement. We thank Lars Ottemöller for critically reading this manuscript and for giving valuable suggestions for improvements.

References

Aristotle University of Thessaloniki, (1981). Aristotle University of Thessaloniki Seismological Network. International Federation of Digital Seismograph Networks, https://doi.org/10.7914/SN/HT.

Aliaj, S. (1998). Neotectonic structure of Albania, J. of Nat. Tech. Sci, (JNTS) 4, 15-42.

Aliaj Sh., 2006. The Albanian orogen: convergence zone between Eurasia and the Adria microplate, In: Pinter N., Grenerczy G., Weber J., Stein S., Medak D. (Eds.), The Adria Microplate: GPS Geodesy, Tectonics and Hazard. NATO Science Series IV-Earth and Environmental Sciences, vol. 61, Springer, 133-149.

Duni, L., N. Kuka and E. Dushi (2003). Monitoring of Seismicity in Albania. EMSC Newsletter 20, 13-16, ISSN 1607-1980.

Dushi, E. (2013). Albanian Broadband Seismological Network design and actual state of the art. SnT2013 Conference, Book of Abstracts, 98, CTBTO, 17-21 June 2013, Vienna, Austria.

Delipetrov, T., K. Blažev, B. Doneva and R. Popovski (2016). Map of the Moho discontinuity of the Republic of Macedonia, Geol. Maced. Special Edition, 4, 2, 493-496.

Dellong, D., F. Klingelhoefer, H. Kopp, D. Graindorge, L. Margheriti, M. Moretti, Sh. Murphy and M. A. Gutscher (2018). Crustal structure of theIonian basin and eastern Sicily margin:Results from a wide-angle seismic survey, J. Geophys. Res.: Solid Earth, 123, 2090-2114.

Dushi, E., R. Koci, E. Begu, Rr. Bozo (2018). Stress inversion from focal mechanism of moderate earthquakes in Albania, SGEM2018 Conference Proceedings, 18, 1.1, 989-996.

D'Agostino, N., M. Métois, R. Koci, Ll. Duni, N. Kuka, A. Ganas, I. Georgiev, F. Jouanne, N. Kaludjerovic, R. Kandić (2020). Active crustal deformation and rotations in the southwestern Balkans from continuous GPS measurements, Earth Planet. Sci. Lett., 539, 116246.

Dushi, E., B. Schurr, E. Kosari, H. Soto, O. Gjuzi, A. Rohnacher, C. Haberland, A. Rietbrock, F. Tilmann, M. Handy, R. Koci, K. Ustaszewski, T. Dahm, T. Meier, and L. Duni (2020). The 2019 Durrës, Albania earthquake sequence – preliminary results from a post-seismic campaign, EGU General Assembly 2020, Online, 4-8 May 2020, EGU2020-22189.

Ekström, G., M. Nettles and A. M. Dziewonski (2012). The global CMT project 2004-2010: Centroid-moment tensors for 13,017 earthquakes, Phys. Earth Planet. Inter., 200-201, 1-9.

Grad, M., T. Tiira and ESC Working Group (2009). The Moho depth map of the European Plate, Geophys. J. Int., 176, 1, 279-292.

Havskov, J. and L. Ottemöller, (2000). SEISAN earthquake analysis software, Seismol. Res. Lett., 70, 532-534.

Havskov, J. and L. Ottemöller, (2010). Routine processing in earthquake seismology. Springer, 347.

Halpaap, F., S. Rondenay and L. Ottemöller, (2018). Seismicity, deformation, and metamorphism in the Western Hellenic Subduction Zone: New constraints from tomography, J. Geophys. Res., 123, 3000-3026.

Handy, M. R., J. Giese, M. S. Schmid, J. Pleuger, W. Spakman, K. Onuzi, and K. Ustaszewski, (2019). Coupled crust-mantle response to slab tearing, bending, and rollback along the Dinaride-Hellenide orogen, Tectonics, 38, 2803-2828.

Handy, M. R., Schmid, S. M., and P. Briole, (2020). The M 6.4 Albanian earthquake of Nov. 26, 2019 and its relation to structures at the Dinarides-Hellenides junctions, Online EGU General Assembly 2020, 4-8, EGU2020-5409.

Havskov, J., P. Voss and L. Ottemöller (2020). Seismological observatory software: Thirty years of SEISAN, Seismol. Res. Lett., 91, 1846-1852.

Institute of Geosciences, Energy, Water and Environment (2002). Albanian Seismological Network. International Federation of Digital Seismograph Networks. https://doi.org/10.7914/SN/AC.

International Seismological Centre (2021), On-line Bulletin, https://doi.org/10.31905/D808B830.

Jouanne, F., L. J. Mugnier, R. Koci, S. Bushati, K. Matev, N. Kuka, I. Shinko, S. Kociaj and L. Duni (2012). GPS constrains on current tectonics of Albania, Tectonophys., 554, 50-62: DOI: 10.1016/j.tecto.2012.06.008.

Kissling, E., U. Kradolfer and H. Maurer (1995).VELEST user's guide-short introduction, Techn. Rep., Institute of Geophysics, ETH Zürich, Switzerland.

Lienert, R. B., E. Berg and N. L. Frazer (1986). HYPOCENTER: An earthquake location method using centered, scaled, and adaptively damped least squares, Bull. Seismol. Soc. Am., 76, 3, 771-783.

Lienert, R. B. and J. Havskov, (1995). A Computer Program for Locating Earthquakes both Locally and Globally, Seismol. Res. Lett., 66, 5, 26-36.

Lentas, K., D. Di Giacomo, J. Harris and A. D. Storchak, (2019). The ISC Bulletin as a comprehensive source of earthquake source mechanisms, Earth Syst. Sci. Data, 11, 565-578.

Lekkas, E., S. Mavroulis, D. Papa, P. Carydis, (2019). The November 26, 2019 Mw 6.4 Durrës (Albania) earthquake. Newsletter of Environmental, Disaster and Crises Management Strategies, 15, ISSN 2653-9454.

Muço, B., (1994). Focal mechanism solutions for Albanian earthquakes for the years 1964-1988, Tectonophys., 231.311-323.

Muço, B., (1995). Some features of seismicity of Albania, Acta Geophys. Polonica, XLIII, 313-324.

Muço, B., (1996). Albanian Seismological Network and its efficiency on recording of the seismic activity of the country. Big Cities World Conference on Natural Disaster Mitigation in conjunction with the 10th International Seminar on earthquake prognostics, Cairo, Egypt, 5-10 January 1996.

Muço, B., (1998). Local Seismological Network and Seismicity of Albania: Twenty years of monitoring. 8-th International IAEGE Congress. Balkema, Rotterdam. In: Morre, D., and O. Hungr (Editors). Engineering Geology: A global view from the Pacific Rim. 1998, ISBN 90-5410-990-4, 797-800.

Muço, B., (1999). Twenty years recording of Albanian Seismological Network: a catalogue and distribution of seismic energy released. In: Wenzel, F., (Editor), Kluwer Academic Publishers, Vrancea Earthquakes: Tectonics, Hazard and Risk Mitigation, 49-56.

Muço, B., F. Vaccari, G. Panza and N. Kuka, (2002). Seismic zonation in Albania using a deterministic approach, Tectonophys., 244, 277-288.

Meço, S., S. Aliaj, I. Turku, (2000). Convergence between the orogen and the Adria microplate, In book: Geology of Albania, 167-168. Gebruder Borntraeger. Berlin. Stuttgart.

Mihaljević, J., P. Zupančič and N. Kuka (2017). BSHAP seismic source characterization models for the Western Balkan region, Bull. Earthquake Eng. 15, 3963-3985.

Moshou A., E. Dushi and P. Argyrakis, (2019). A preliminary report on the 26 November 2019, M = 6.4 Durrës, Abania Earthquake, EMSC Reports, https://www.emsc-csem.org/Files/news/Earthquakes_reports.

Mavroulis, S., E. Lekkas, P Carydis (2021). Liquefaction Phenomena Induced by the 26 November 2019, Mw = 6.4 Durrës (Albania) Earthquake and Liquefaction Susceptibility Assessment in the Affected Area, Geosciences 2021, 11, 215.

MedNet Project Partner Institutions. (1990). Mediterranean Very Broadband Seismographic Network (MedNet). Istituto Nazionale di Geofisica e Vulcanologia (INGV). https://doi.org/10.13127/SD/fBBBtDtd6q.

Ormeni, Rr. (2009). Crustal structures beneath the seismogenic zones and lateral velocity contrasts across deep faults of Albania, Journal of the Balkan Geophysical Society, 12, 1, 1-8.

Ormeni, R., (2011). P, S wave velocity model of the crust and uppermost mantle of Albania region, Tectonophysics, 497, 114-121.

Peci, V., and S. Shubleka, (2001). A new elaboration of earthquakes on Albania and surrounding area for the period 1964-1995. The Albania, J. of Nat. Tech. Sci. (JNTS), 10, 35-42.

Papazachos, C., E. Scordilis, V. Peci (2002). P and S Deep Velocity Structure of the Southern Adriatic-Eurasia Collision Zone Obtained By Robust Non-linear Inversion of Travel Times. EGS General Assembly Conference Abstracts (2002EGSGA...27.6553P).

Papadopoulos, G. A., A. Agalos, P. Carydis, E. Lekkas, S. Mavroulis and L. Triantafyllou, (2020). The 26 November 2019 Mw 6.4 Albania Destructive Earthquake, Seismol. Res. Lett., XX, 1-10.

Sector for Seismology, Institute of Hydrometeorology and Seismology of Montenegro. (1982). Montenegrin Seismic Network [Data set]. International Federation of Digital Seismograph Networks. https://doi.org/10.7914/SN/ME.

Stipčević, J., H. Tkalčić, M. Herak, D. Markušić and D. Herak, (2011). Crustal and uppermost mantle structure beneath the External Dinarides, Croatia, determined from teleseismic receiver functions, Geophys. J. Int., 185, 3, 1103-1119.

Storchak, D. A., J. Harris, L. Brown, K. Lieser, B. Shumba and D. Di Giacomo, (2020). Rebuild of the Bulletin of the International Seismological Centre (ISC)—part 2: 1980-2010, Geosci. Lett. 7: 18.

***CORRESPONDING AUTHOR: Edmond DUSHI**,
Department of Seismology, Institute of Geosciences, Polytechnic University of Tirana, Albania
e-mail: e.dushi@geo.edu.al